Наносистеми, наноматеріали, нанотехнології
Nanosistemi, Nanomateriali, Nanotehnologii
2026, т. 24, № 1, сс. 189–200
https://doi.org/10.15407/nnn.24.01.0189

PACS numbers: 68.37.Hk, 68.37.Vj, 68.55.A-, 78.20.Ci, 78.40.Fy, 78.67.-n, 81.15.Rs

Study of the Optical and Structural Properties of Cadmium-Oxide Thin Films Prepared Using Chemical Spray Pyrolysis Technique

Mohammed S. Sinjar and Mushtaq Abed Al-Jubbori

College of Education for Pure Sciences,
Department of Physics,
University of Mosul,
41001 Mosul, Iraq

Cadmium oxide (CdO) thin films are synthesized by the chemical spray pyrolysis method on glass. The thin-film substrates are prepared at varying temperatures: 400°C, 450°C, 500°C. The samples are examined using a double beam spectrometer UV–Vis; the absorbance and reflectance spectra of the produced films are measured over a range of wavelengths 310–910 nm in order to study the optical properties of these films. As discovered, the absorbance varies with wavelength. Specifically, we observe that the absorbance behaves in the opposite direction of the transmittance, peaking at 350 nm, after which the absorbance spectrum starts to decay exponentially until the absorbance hits its lowest value at the 700 nm wavelength. The results reveal absorbance spectrum achieving its maximum value at 400°C and lowest value at 500°C. As also observed, the value of the spectrum remains consistent within the range of 700–910 nm; the evaluated energy band gap increases from 2.33 eV to 2.41 eV with the increase of substrate temperature. Furthermore, the results for the optical constants such as the refractive index, extinction coefficient, and absorption coefficient decrease with substrate temperature.

Тонкі плівки оксиду Кадмію (CdO) було синтезовано методом хемічної розпорошувальної струминної піролізи на склі. Тонкоплівкові підкладинки було підготовлено за різних температур: 400°C, 450°C, 500°C. Зразки було досліджено за допомогою двопроменевого UV–Vis-спектрометра; спектри вбирання та відбивання одержаних плівок було виміряно в діяпазоні довжин хвиль 310–910 нм задля вивчення оптичних властивостей цих плівок. Було виявлено, що вбирання змінюється з довжиною хвилі. Зокрема, ми спостерігаємо, що вбирання поводиться протилежним чином щодо пропускання, досягаючи піку при 350 нм, після чого спектер вбирання починає експоненційно спадати, поки вбирання не досягне свого найнижчого значення за довжини хвилі у

700 нм. Результати показали, що спектер вбирання досяг свого максимального значення при 400°C, а найнижчого значення — при 500°C; також було відзначено, що значення спектру залишається стабільним у діяпазоні 700–910 нм, а оцінена ширина забороненої зони збільшується з 2,33 еВ до 2,41 еВ зі збільшенням температури підкладинки. Крім того, результати стосовно оптичних констант, таких як показник заломлення, коефіцієнт екстинкції та коефіцієнт вбирання, зменшуються з температурою підкладинки.

Key words: cadmium oxide, chemical spray pyrolysis, energy gap, absorbance spectrum.

Ключові слова: оксид Кадмію, хемічна розпорошувальна струминна піроліза, заборонена енергетична зона, спектер вбирання.

(Received 30 September, 2024; in revised form, 18 October, 2024)

1. INTRODUCTION

Recent years have seen a significant increase in interest in transparent conducting oxides (TCO) thin films due to their distinct chemical and physical characteristics that set them apart from bulk materials and individual atoms. Because of its uses in optoelectronic devices like solar cells, phototransistors and diodes, transparent electrodes, and gas sensors, researchers have turned their attention to cadmium oxide (CdO) in recent years [1].

Large energy band gaps (bulk CdO is an *n*-type broad band gap semiconductor with a direct band gap of 2.3 eV and an indirect band gap of 1.36 eV), a high transmission coefficient in the visible spectral domain, and remarkable luminescence characteristics are just a few of the materials' many appealing qualities that make CdO thin films appealing.

Over the past decade, numerous techniques have been employed to prepare CdO thin films, including spray pyrolysis [2], oxidation of cadmium films [3], metal organic chemical vapour deposition (MOCVD) [4], sol–gel [5], sputtering [6], vacuum evaporation [7], and reactive pulsed laser deposition [8]. These techniques have all been studied for their electrical and optical properties. It was demonstrated through experimentation that these characteristics are highly dependent on the deposition circumstances and film structure. The size and form of the particles, in addition to deviations from the ideal CdO stoichiometry, determine the intensity of the optical and electrical effects of CdO.

The primary impacts of UV irradiation on thin films are alterations in their thickness, chemical composition, and structure, which result in changes to their electrical and optical properties, accord-

ing to several recent researches [9–12]. When silicon oxide thin films were exposed to airborne UV light, Bradford *et al.* [11, 12] noticed changes in the films' optical characteristics and explained these changes as the result of an increase in oxygen molecules or atoms in the deposited films. Electrons are excited by UV light and move from the valence to the conduction band, creating holes in the process. Redox interactions with the surface species can be started by the photogenerated electron–hole pairs that move to its surface [10, 13, 14]. When TiO_2 films are subjected to UV irradiation, two distinct and independent processes take place, according to Fernández–Rodríguez *et al.* [10]: changes in the contact angle. These alterations mostly impact the film surfaces, and the majority of the material is probably going to undergo oxygen incorporation and rearrangement. We are curious as to whether these changes brought about by UV irradiation might also have an impact on its other characteristics. This research aims to examine how UV irradiation affects the optical characteristics and structure of CdO thin films.

CdO films can be grown using a variety of methods, including thermal evaporation [5], sputtering [6], pulsed laser deposition [7], molecular beam epitaxy [8], spray pyrolysis [4], and metal organic chemical vapour deposition (MOCVD) [9, 10]. However, despite its great promise, the formation of films thinner than 100 nm of this material has not been well studied, that is, to the best of our knowledge, and no results have been found in the literature as of yet. The paucity of reports may be explained by the challenges in regulating the growth parameters to promote lateral development when growing into substrates [11], where flat surfaces with varying growth rates are essential.

However, because of their unique nucleation characteristics and the lack of a substantial number of nucleation sites on the substrate, some research on the growth of this material reveals the challenges in obtaining high densities of isolated nanoparticles of CdO on substrates [12]. Some growth restrictions on flat thin layers with good crystalline quality may also stem from this challenge.

2. EXPERIMENTAL DETAILS

2.1. Sample Preparation

The process of preparing CdO solution is done using cadmium acetate [$(CH_3COO)_2Cd_2H_2O$] [M.W. = 266.53 gm/m]. It is a white powder of American origin provided by (SIGMA CHEMICAL CO). To prepare a solution with a concentration of 0.1 M at room temperature, 2.6653 gm is dissolved using a sensitive four-level electronic balance of cadmium acetate to be dissolved in 100 mL of distilled water and the

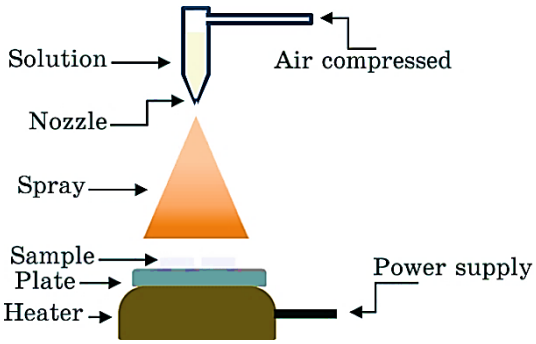

Fig. 1. Experimental setup of the spray pyrolysis technique.

two materials are mixed well using a magnetic stirrer at a temperature of 40°C for 10 min to ensure the homogeneity of the solution, which results in a colourless solution like water. Then, the solution is filtered through filter paper to obtain a clear solution without any sediments or possible impurities. Square glass slides with dimensions of 2.5 cm and an area of 6.25 cm^2 are used, where they are cleaned well in three stages to ensure obtaining completely clean slides. These three stages begin by cleaning them using running water with soap solution for 3 min to remove traditional dirt, then immersing them in acetone and placing them in the ultrasonic device for 15 min, and finally washing them with distilled water and then drying them using hot air for 120 sec.

The prepared substrates are placed on the surface of an electric heater to obtain the required temperature as shown in Fig. 1. The deposition time is set at 10 sec at a rate of 20 sprays with a 3 min pause between each two sprays. The vertical distance between the nozzle of the spray device and the glass substrate is 30 cm and the temperature of the substrates is fixed at 400, 450, and 500°C and a total of 20 sprays for each temperature. The air pressure is set at 2 bars. The details of the spraying process are mentioned in Table.

3. RESULTS AND DISCUSSIONS

3.1. The Optical Absorption Analysis

The interaction of light with CdO thin films was studied to learn more about the optical properties. We used UV–Vis spectroscopy (Shimadzu UV-1800) to characterize the optical properties of CdO thin films at a scanning rate of 400 nm/min and the absorption spectra were obtained from 190–1100 nm). When light interacts with the thin film, an optical absorption process occurs against the

TABLE. Parameters for the spray deposition of the films.

Spray parameters	Optimum value/item
$(CH_3COO)_2Cd_2H_2O$ solution concentration	0.1 M
Nozzle	Glass
Nozzle–substrate distance	30 cm
Solvent	Distilled water
Carrier gas	Compressed air
Pressure	2 bar
Solution flowrate	5 mL/min
Substrate temperature	400, 450, 500°C

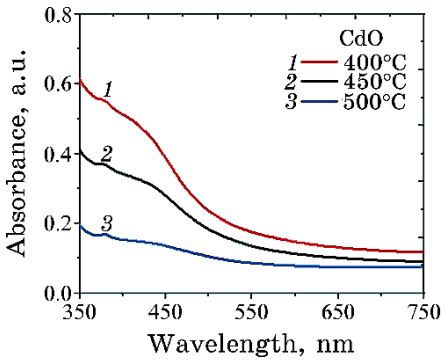

Fig. 2. UV–Vis absorbance curves of CdO films as a function of substrate temperature.

wavelength spectra of the thin films deposited at different temperatures of the glass substrates on which they were deposited. Figure 2 shows a decrease in absorption with increasing temperature. The spectra also showed a clear decrease in absorption at long wavelengths, indicating the presence of direct optical transition in the thin films, as well as a shift to red with increasing temperatures of the glass substrates. High temperatures can affect structural properties such as crystallinity, grain size, and defect density, which in turn affect the optical behaviour of the material.

The surface plasmon resonance (SPR) peak of CdO thin films on glass was observed at 350 nm. The peak shape is due to the light scattering caused by the CdO thin films and the peak position due to the absence of agglomeration in the nanoparticles deposited on the glass and the interactions between CdO particles and different substrates. It is worth noting that the UV–Vis spectrum of CdO nanoparticles on glass substrate shows only the SPR peak corresponding to the in-plane dipole. Crystallization is enhanced at higher temperatures during the

growth of the thin film better, the density of defects such as grains and dislocations decreases and, as a result, the light absorption by these defects decreases. This in turn leads to a decrease in the overall absorption. Higher temperatures can also facilitate the growth of smoother film surfaces by enhancing the mobility and diffusion of nanoparticles on the surface. Reducing the surface roughness reduces light scattering and increases the light transmission through the film. This also leads to a decrease in absorption. The colour of the CdO film changes from light brown to dark brown with increasing temperature of the glass substrates.

The incident photon energy as well as the properties of the material itself have an impact on a materials' absorption coefficient. According to Beer's law, the transmission (T) and reflection (R) spectra are related to the absorption coefficient [12]:

$$\alpha = \frac{1}{d}\log\left[\frac{(1-R)^2}{2T} + \frac{(1-R)^2}{\sqrt{2T^2+R^2}}\right], \tag{1}$$

where d is the thickness of the sample. The absorption coefficient (α) at the wavelength of maximum absorption decreases with the increased substrate temperatures of CdO thin films as shown in Fig. 3.

An important factor affecting a materials' optical and electronic properties is the optical band gap $E_g^{opt.}$. The optical band gap of the CdO thin films was determined using the Tauc plot and calculated by fitting the equation to the data of Ref. [13]:

$$(\alpha h\nu)^{1/2} = k\left(h\nu - E_g^{opt.}\right), \tag{2}$$

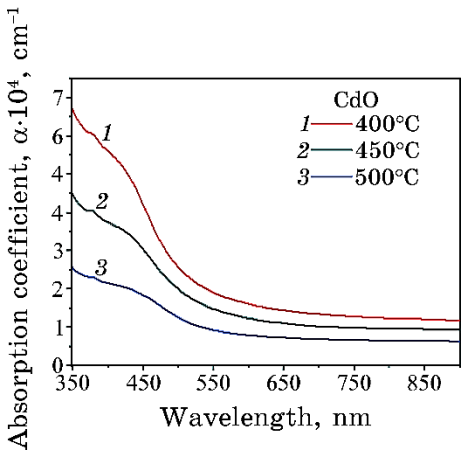

Fig. 3. Absorption coefficient of CdO thin films as a function of wavelength with difference substrate temperatures.

where r is a number that indicates the type of electronic transition that causes the absorption and takes values of 1/2 or 2/3 for direct transitions and 2 or 3 for indirect ones, depending on whether the transition is allowed or forbidden, respectively. $h\nu$ is the photon energy; α is the absorption coefficient, and B is a constant of effective mass. Figure 4 presents the optical energy gap increasing with increasing substrate temperatures.

The refractive index (n) describes how a beam propagates through a transparent medium. The optical parameters of the samples can be used to determine the refractive index using the following relationship [14]:

$$n = \left(\frac{1+R}{1-R}\right) + \sqrt{\frac{4R}{(1-R)^2} - K^2}\,. \tag{3}$$

Reflectivity (R) is calculated from absorption and transmission spectra using the law of conservation of energy [$R = 1 - T - A$]. On the other hand, the extinction coefficient (K) depends on the absorption coefficient and wavelength of the incident beam and is given by [15]

$$K = \frac{\alpha\lambda}{4\pi}\,. \tag{4}$$

The refractive index and the extinction coefficient against wavelength are given in Eq. (3) and Eq. (4). It can be seen that n and K of CdO thin films decreases with increasing substrate temperatures, and, in the visible region, when thin films are deposited onto a sub-

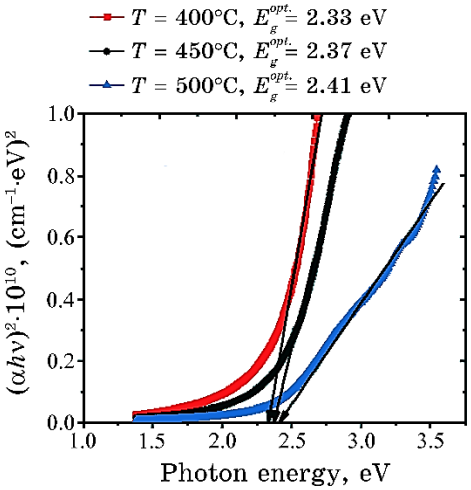

Fig. 4. Optical band gap values for prepared CdO thin films for different substrate temperatures.

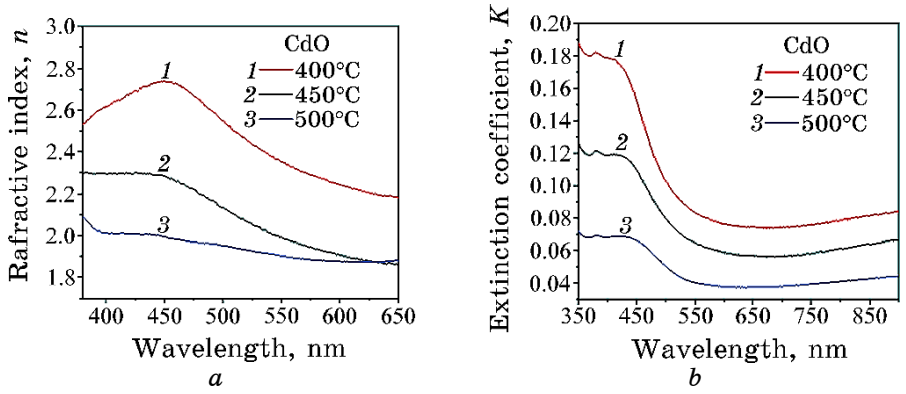

Fig. 5. Refractive index (*a*) and extinction coefficient (*b*) as a function of wavelength for CdO thin films for different substrate temperature.

strate at higher temperatures, they tend to have improved crystallinity and reduced defects. In the case of CdO thin films, increasing the substrate temperature can lead to better crystallization and larger grain sizes, which can result in reduced light scattering and absorption. This, in turn, leads to a decrease in both the refractive index and extinction coefficient as displayed in Fig. 5.

The complex dielectric constant caused by photon interactions with medium charges is commonly referred to as polarization. Using Maxwell's relations, evaluation the real (ε_r) and imaginary (ε_i) parts of the dielectric constant can be calculated for optical wavelengths based on optical constants. The refractive index and extinction coefficient are connected to the real and imaginary of the dielectric constant through the following relationships [16]:

$$\varepsilon_r = n^2 - K^2, \ \varepsilon_i = 2nK. \tag{5}$$

The real and imaginary dielectric constants of CdO thin films decrease with increasing substrate temperatures and in the visible region as are plotted in Fig. 6. Nanoparticles size in CdO thin films can be affected by increasing the substrate temperature. The materials' dielectric properties are impacted by changes in bandgap and carrier concentration, as, especially in the visible range. Consequently, the real and imaginary dielectric constants decrease.

The optical conductivity CdO thin films can be determined using the correlation between the absorption coefficient and the refractive index [16]:

$$\sigma_{opt.} = \frac{\alpha nc}{4\pi}, \tag{6}$$

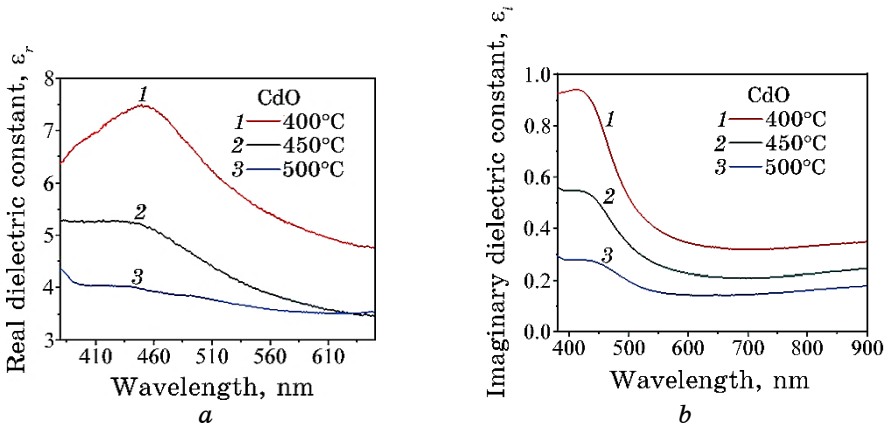

Fig. 6. Real dielectric constants (*a*) and imaginary dielectric constants (*b*) as functions of wavelength for CdO thin films for different substrate temperature.

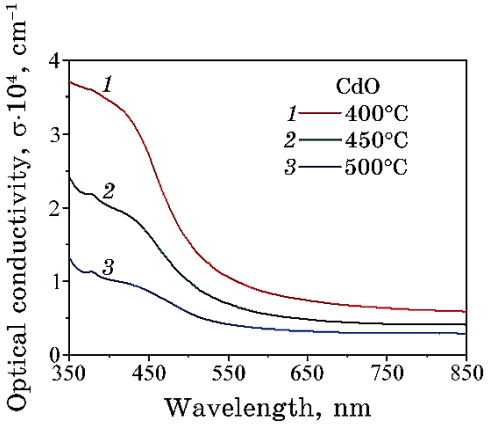

Fig. 7. Optical conductivity as a function of wavelength for CdO thin films for different substrate temperature.

where c is the speed of light in a vacuum. The decrease in optical conductivity can be attributed to decrease for absorption coefficient and the refractive index with increasing the substrate temperature, as shown in Fig. 7.

3.2. Field Emission–Scanning Electron Microscopy (FE–SEM) Results

Utilizing the FE–SEM analysis at a 200k× magnification, it possible to analyse the morphology and particle size distribution of CdO thin

films for different substrate temperature.

With increasing substrate temperature, the nanoparticles of CdO become larger due to the heightened kinetic energy of the particles, rendering them more susceptible to diffusion and coalescence, leading to the formation of larger particles. Consequently, a denser and less porous membrane is formed, exhibiting greater cohesion. More-

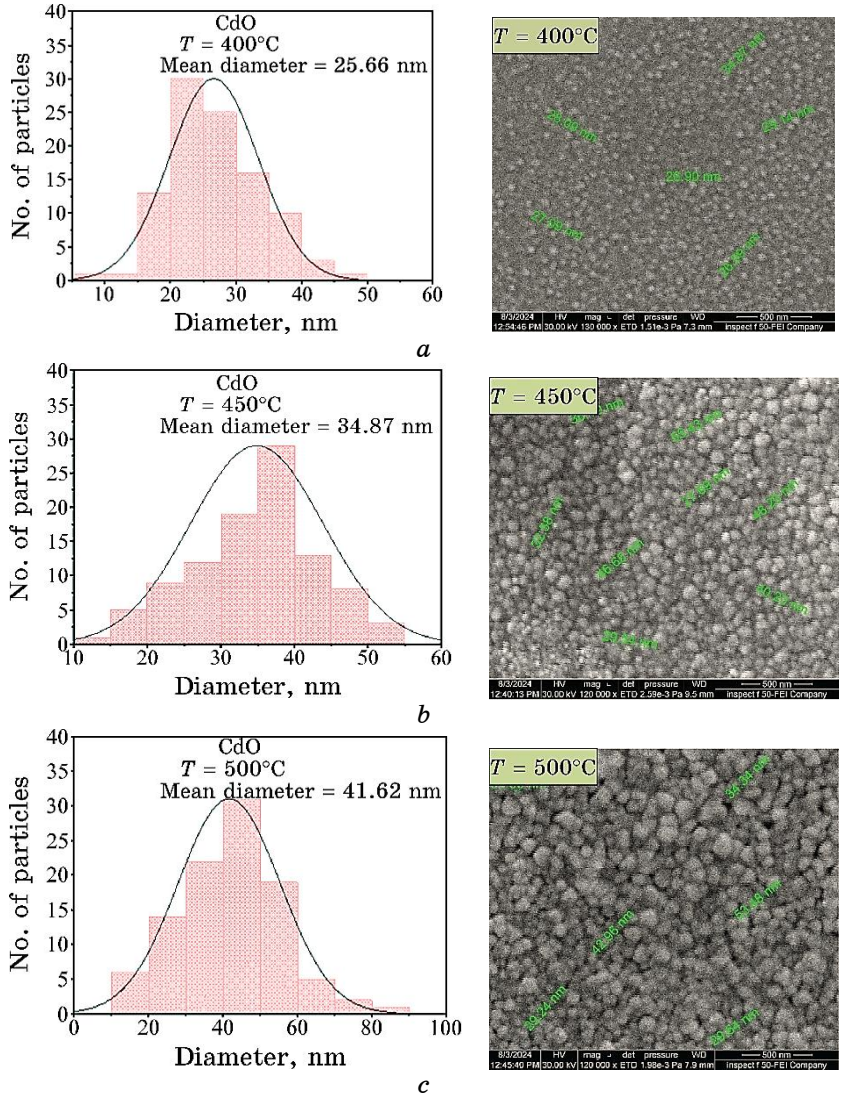

Fig. 8. FE–SEM micrographs of CdO thin films for different substrate temperature and the particle size distribution for (*a*) 400°C, (*b*) 450°C, and (*c*) 500°C.

over, the shape of the membrane particles is also affected, as the particles tend to become more spherical with increasing substrate temperature. This is because of the increasing in temperature reduces the surface tension on the membrane particles, allowing them to adopt a more stable shape.

The FE–SEM images in Fig. 8 clearly show that CdO-nanoparticles' diameters with a size range of 25, 34, and 41 nm for 400, 450, and 500°C, respectively. Finally, the FE–SEM results are in good agreement with the results of UV–Vis analysis.

4. CONCLUSIONS

Cadmium oxide thin films can be easily and low-cost produced by chemical spray pyrolysis technique. The optical properties show that the optical constants such as refractive index, extinction coefficient, dielectric constants and optical conductivity decreases with increasing substrate temperature. In addition, the surface morphology of CdO thin films is a sphere-like shape and diameters increasing with substrate temperature. The average particles size range of 25, 34 and 41 nm for 400, 450, and 500°C, respectively.

ACKNOWLEDGEMENTS

The authors would like to express their warmest thanks to the University of Mosul, College of Education for Pure Science, Department of Physics for supporting this work.

REFERENCES

1. Yoon-Heung Tak, Ki-Beom Kim, Hyoung-Guen Park, Kwang-Ho Lee, and Jong-Ram Lee, *Thin Solid Films*, **411**, Iss. 1: 12 (2002); https://doi.org/10.1016/S0040-6090(02)00165-7
2. Seval Aksoy, Yasemin Caglar, Saliha Ilican, and Mujdat Caglar, *Int. J. Hydrogen Energy*, **34**, Iss. 12: 5191 (2009); https://doi.org/10.1016/j.ijhydene.2008.09.057
3. C. Danţuş, G. G. Rusu, M. Dobromir, and M. Rusu, *Appl. Surf. Sci.*, **255**, Iss. 5: 2665 (2008); https://doi.org/10.1016/j.apsusc.2008.07.176
4. Antonino Gulino and Giovanni Tabbi, *Appl. Surf. Sci.*, **245**, Iss. 1–4: 322 (2005); https://doi.org/10.1016/j.apsusc.2004.10.026
5. D. M. Carballeda-Galicia, R. Castanedo-Pérez, O. Jiménez-Sandoval, S. Jiménez-Sandoval, G. Torres-Delgado, and C. I. Zúciga-Romero, *Thin Solid Films*, **371**, Iss. 1–2: 105 (2000); https://doi.org/10.1016/S0040-6090(00)00987-1
6. Qiang Zhou, Zhenguo Ji, BinBin Hu, Chen Chen, Lina Zhao, Chao Wang, *Mater. Lett.*, **61**, Iss. 2: 531 (2007); https://doi.org/10.1016/j.matlet.2006.05.004
7. A. A. Dakhel and F. Z. Henari, *Cryst. Res. Technol.*, **38**, Iss. 11: 979 (2003);

https://doi.org/10.1002/crat.200310124
8. Raid A. Ismail, Bassam G. Rasheed, Evan T. Salm, and Mukram Al-Hadethy, *J. Mater. Sci.: Mater. Electron.*, **18**: 1027 (2007); https://doi.org/10.1007/s10854-007-9129-4
9. Khalaf Ajaj, Abdullah M. Ali, and Mushtaq Abed Al-Jubbori, *Nanosistemi, Nanomateriali, Nanotehnologii*, **22**, Iss. 1: 209 (2024); https://doi.org/10.15407/nnn.22.01.209
10. M. Fernández-Rodríguez, V. J. Rico, A. R. González-Elipe, and A. Álvarez-Herrero, *phys. stat. sol. (c)*, **5**: 1164 (2008); https://doi.org/10.1002/pssc.200777790
11. A. P. Bradford, G. Hass, M. McFarland, and E. Ritter, *Appl. Opt.*, **4**, Iss. 8: 971 (1965); https://doi.org/10.1364/AO.4.000971
12. Alan P. Bradford and Georg Hass, *J. Opt. Soc. Am.*, **53**: 1096 (1963); https://doi.org/10.1364/JOSA.53.001096
13. Yunxia Wang, Hongling Wang, and Fengyuan Yan, *Surf. Interface Anal.*, **41**, Iss. 5: 399 (2009); https://doi.org/10.1002/sia.3039
14. Kenichi Katsumata, Akira Nakajima, Tadashi Shiota, Naoya Yoshida, Toshiya Watanabe, Yoshikazu Kameshima, and Kiyoshi Okada, *J. PhotoChem. Photobiol. A*, **180**, Iss. 1–2: 75 (2006); https://doi.org/10.1016/j.jphotochem.2005.09.023
15. M. Zaien, N. M. Ahmed, and Z. Hassan, *Mater. Lett.*, **105**: 84 (2013); https://doi.org/10.1016/j.matlet.2013.04.070
16. Q. Zhou, Z. Ji, B. Hu, C. Chen, L. Zhao, and C. Wang, *Mater. Lett.*, **61**: 531 (2007); http://dx.doi.org/10.1016/j.matlet.2006.05.004
17. B. J. Zheng, J. S. Lian, L. Zhao, and Q. Jiang, *Vacuum*, **85**, Iss. 9: 861 (2011); http://dx.doi.org/10.1016/j.vacuum.2011.01.002
18. A. B. M. A. Ashrafi, H. Kumano, I. Suemune, Y. W. Ok, and T. Y. Seong, *J. Cryst. Growth*, **237–239**: 518 (2002); http://dx.doi.org/10.1016/S0022-0248(01)01956-X
19. L. C. S. Murthy and K. S. R. K. Rao, *Bull. Mater. Sci.*, **22**: 953 (1999); https://doi.org/10.1007/BF02745685
20. J. Zúniga-Pérez, C. Martínez-Tomás, and V. Munoz-Sanjosé, *physica status solidi (c)*, **2**, Iss. 3: 1233 (2005); http://dx.doi.org/10.1002/pssc.200460672
21. D. Lamb and S. J. C. Irvine, *Thin Solid Films*, **518**, Iss. 4: 1222 (2009); https://doi.org/10.1016/j.tsf.2009.05.067
22. Y. J. Chen, Y. Y. Shih, C. H. Ho, J. H. Du, and Y. P. Fu, *Ceram. Int.*, **36**, Iss. 1: 69 (2010); http://dx.doi.org/10.1016/j.ceramint.2009.06.018
23. Sreekumar Rajappan Achary, Said Agouram, Juan F. Sánchez-Royo, M. Carmen Martínez-Tomás, and Vicente Mucoz-Sanjosé, *RSC Adv.*, **4**, Iss. 44: 23137 (2014); http://dx.doi.org/10.1039/c4ra01818d
24. Isha Saini, Jyoti Rozra, Navneet Chandak, Sanjeev Aggarwal, Pawan K. Sharma, and Annu Sharma, *Materials Chemistry and Physics*, **139**, Iss. 2–3: 802 (2013); https://doi.org/10.1016/j.matchemphys.2013.02.035
25. J. Tauc, R. Grigorvici, and A. Vancu, *physica status solidi (b)*, **15**, Iss. 2: 627 (1966); https://doi.org/10.1002/pssb.19660150224
26. M. Rashidian and D. Dorranain, *J. Theor. Appl. Phys.*, **8**: Article No. 121 (2014); https://doi.org/10.1007/s40094-014-0121-0
27. A. Kurt, *Turkish Journal of Chemistry*, **34**, Iss. 1: 67 (2010); https://doi.org/10.3906/kim-0903-29
28. Dinesh Babu K, Philominathan P, and Murali K, *Optik*, **186**, Iss. 3: 350 (2019); https://doi.org/10.1016/j.ijleo.2019.03.048